

EVIDENCE OF DYNAMICAL COUPLING BETWEEN THE RESIDUAL LAYER AND THE DEVELOPING CONVECTIVE BOUNDARY LAYER

G. JAVIER FOCESATTO[†] and PHILIPPE DROBINSKI

Laboratoire de Météorologie Dynamique, École Polytechnique, Palaiseau, France

CYRILLE FLAMANT

Service d'Aéronomie, Université Pierre et Marie Curie, Paris, France

DANIEL GUEDALIA and CLAIRE SARRAT

Laboratoire d'Aérodynamique, Université Paul Sabatier, Toulouse, France

PIERRE H. FLAMANT

Laboratoire de Météorologie Dynamique, École Polytechnique, Palaiseau, France

JACQUES PELON

Service d'Aéronomie, Université Pierre et Marie Curie, Paris, France

Abstract. The diurnal cycle of the atmospheric boundary layer (ABL) has been documented on 8 August 1998 in the framework of the Étude et Simulation de la Qualité de l'air en Ile-de-France (ESQUIF) experiment that took place in the Paris area. The ABL dynamics was documented by means of a ground-based lidar, surface meteorological stations and soundings. The interaction between the residual layer and the convective boundary layer is investigated using the collected data as well as mesoscale modeling. As opposed to the generally accepted concept, we find evidence of entrainment at the top of the residual layer. High temporal simulations of the 8 August 1998 case made with the mesoscale atmospheric model Meso-NH also evidence mixing at the top of the residual layer (RL). This mixing is believed to be related to the presence of convective (gravity) waves in the RL.

Keywords: Residual layer, convective boundary layer, vertical coupling, lidar, non-hydrostatic modeling

1. Introduction

The residual layer (RL) is a neutrally stratified layer which does not have direct contact with the ground, and is not affected by turbulent transport of surface related properties (as opposed to the convective boundary layer where this transport is ensured by thermals). In the RL, transport is ensured by shear-related sporadic bursts of turbulence (Mahrt, 1999). RL characteristics (mean state and concentration vari-

[†] G. Javier Fochesatto is also with CEILAP (CITEFA-CONICET), villa Martelli, Argentina



ables) are generally observed to be initially the same as those of the recently decayed mixed layer (Stull, 1988). In the absence of vertical transport by thermals, the height of the top of the RL is expected to be constant overnight (if we except the effect of subsidence and radiative cooling) until fully eroded by the developing convective boundary layer (CBL). Until now, this "conceptual" scheme has not been invalidated, even though adapted observation tools, such as remote sensing instruments, have been used for ABL studies for the past 30 years (see Wilczak et al., 1996 for example).

As there is now convincing evidence that RLs have an impact on air quality, via down-mixing of pollutants during the growth of the mixing layer in the morning (Neu et al., 1994; among others), numerous studies have reported lidar measurements of the ABL evolution in the daytime, especially in urban areas (Drobninski et al., 1998; Dupont et al., 1999; Menut et al., 1999; among others). In contrast, only a few studies have been conducted on the nocturnal boundary layer using lidars (Devara et al., 1994; Raj et al., 1997; Di Girolamo et al., 1999; Kolev et al., 2000). To the author's knowledge, only the transition from the daytime to nighttime boundary layer regime has been investigated (Mahrt, 1981; Nieuwstadt and Brost, 1986; Kolev et al., 2000). No studies have been devoted to transition from nocturnal to convective boundary layer, in general, and to the interaction between the RL and the CBL, in particular.

In this paper, we present evidence of dynamic coupling between the RL and the developing CBL as observed by ground-based backscatter lidar in the framework of the Étude et Simulation de la QUalité de l'air en Ile-de-France (ESQUIF) experiment (Menut et al., 2001) in the area of Paris (France). This phenomenon has been observed in each of the clear air intensive observation periods (IOP's) of ESQUIF that have been analysed. Here, we report on the 8 August 1998 case (IOP 2). High temporal simulations of the 8 August 1998 case made with the mesoscale atmospheric model Meso-NH (Lafore et al., 1998) also evidence mixing at the top of the RL.

2. The 8 August 1998 case study

The highest pollution levels of the summer of 1998 were recorded during IOP 2. During the first two weeks of August, photo-oxidant pollution was favoured by high temperatures, especially during a four-day long heatwave (from 8 to 11 August 1998), with air temperatures near the surface ranging from 35 to 37°C. On 8 August 1998, winds were from the East over the Paris area with negligible subsidence (see below). At

10 m above ground level, the winds did not exceed $3\text{--}4\text{ m s}^{-1}$. The air masses sampled over Paris had travelled over the British Isles as well as Belgium, the Netherlands and Luxemburg.

2.1. OBSERVATIONS

An upward looking backscatter lidar has been deployed on the instrumented site of Palaiseau (a suburban site located 25 km south of Paris). The lidar is intended to document some of the key parameters relevant to (i) the atmospheric boundary layer (ABL) dynamics i.e. the ABL depth and entrainment zone depth and (ii) radiative budget i.e. optical depth with an accuracy of ± 0.02 . The vertical resolution of the instrument is 30 m. In addition, measurements of infrared and longwave radiations using a pyranometer and a pyrgeometer, and measurements of temperature, humidity and wind velocity and direction were performed simultaneously to lidar measurements on the same site.

2.1.1. *Atmospheric reflectivity*

Recently, lidar measurements of ABL diurnal evolution in the Paris are have been reported by Drobinski et al. (1998), Dupont et al. (1999) and Menut et al. (1999). The backscatter lidar used in this study operates in the visible part of the spectrum (at $0.53\text{ }\mu\text{m}$) and the lidar signal is extremely sensitive to particles with radii between 0.1 and $1\text{ }\mu\text{m}$. Sub-micronic aerosols are excellent tracers of the dynamics in troposphere, making lidar a relevant tool for the study of ABL processes such as entrainment over homogeneous terrain (Flamant et al., 1997), organized-large eddies (Drobinski et al., 1998) and over complex orography (Drobinski et al., 2001). Once they have been stripped from the surface, aerosols are trapped in the ABL by the capping temperature inversion. As a result, the lidar signal is generally observed to be large in the ABL and to decrease rapidly above (Flamant and Pelon, 1996).

Zenith lidar observations on 8 August 1998 were performed over Palaiseau from 0800 to 1700 UTC. The temporal evolution of the ABL (CBL and RL) structure, as obtained from the range-squared-corrected signal, is shown in Figure 1A. The temporal resolution is 25 s. The CBL appears as an orange-red layer (on the false-colour picture) which deepens from 625 to 2400 m between 1000 and 1700 UTC. The RL also appears as an orange-red layer, but above the CBL and between 0800 and 1300 UTC.

2.1.2. *Heights of the residual layer and convective boundary layer*

The top of the CBL is characterized by large gradients of mean quantities, such as the relative humidity and aerosol content, to which the

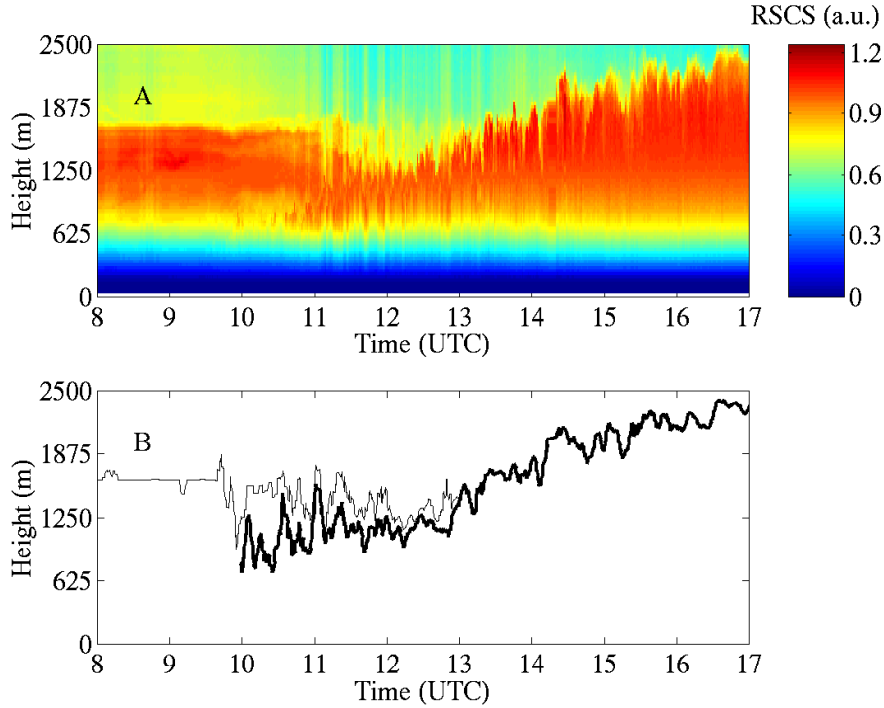


Figure 1. Panel A: Lidar time series over Palaiseau on 8 August 1998 from 0800 to 1700 UTC. The relationship between the range-squared corrected backscatter signal (RSCS in arbitrary units) and color coding is given by the color bar. Panel B: RL (thin solid line) and CBL (thick solid line) top heights (h_{RL} and h_{CBL} , respectively) as a function of time.

backscattered signal is highly sensitive (Dupont et al., 1994). Lidar profiles always exhibit a local discontinuity (or transition zone) between the mixed layer and the troposphere aloft. We define the local CBL top height as the base of the transition zone (i.e. the top of the mixed layer) using a gradient algorithm (Dupont et al., 1994). In this study, it is assigned to the level of the first data point whose backscatter intensity exceeds the free troposphere backscatter intensity by at least 25%. The precision on the so retrieved heights is 30 m. The same algorithm can be used to detect the top of the RL. In the following, these heights are referred to as h_{CBL} and h_{RL} and are displayed as a function of time in Figure 1B. The temporal resolution for h_{CBL} and h_{RL} time series is 25 s.

2.1.3. Soundings

The vertical thermodynamical structure of the atmosphere in the Paris area is documented by means of soundings performed by Météo-France

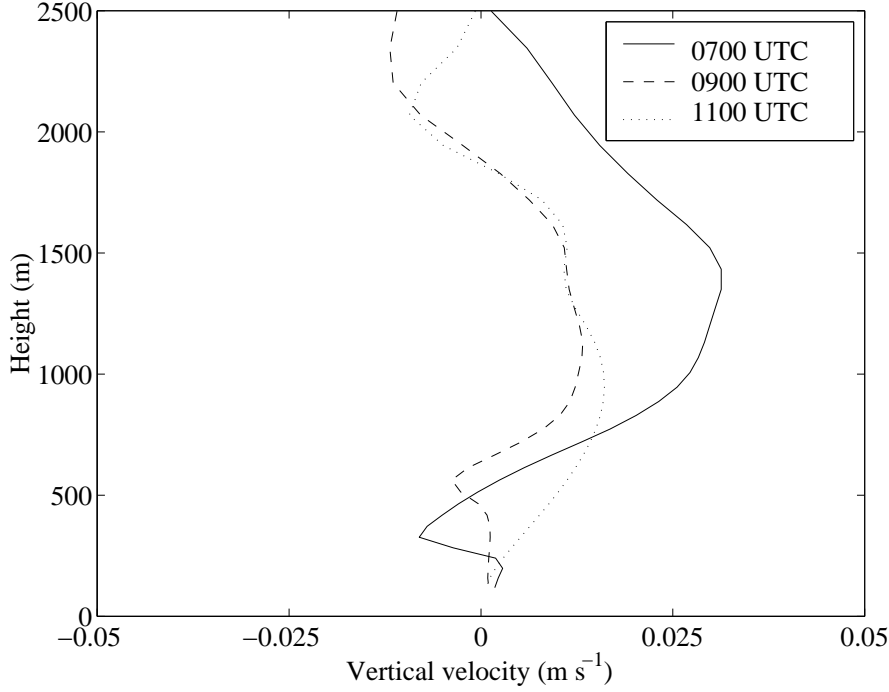


Figure 2. Vertical velocities (from the 3D Meso-NH simulation) over Paris at 0700, 0900 and 1100 UTC (solid, long-dash and short-dash lines, respectively).

in Trappes (25 km southwest of Paris, 15 km away from Palaiseau). Temperature, relative humidity, pressure and wind speed and direction soundings are available at 0000 and 1200 UTC. During IOP's, soundings were performed every three hours. The diurnal evolution of the depth of the ABL can be estimated from potential temperature, relative humidity and wind measurements. It can in turn be compared to that derived from lidar measurements (Menut et al., 1999), as presented in Table I. The relative humidity between 0 and 3 km above ground level remained lower than 40% throughout the day. As a result, the small fluctuations (both on the vertical and with time) of relative humidity will have little influence on the evolution of the size and refractive index of the aerosol, and in turn, little influence on the lidar signal itself (Dupont et al., 1994; Flamant et al., 1998).

2.2. MESOSCALE MODELING

The Meso-NH model (Lafore et al., 1998; Bélair et al., 1998) solves the non-hydrostatic and anelastic equation system. It allows for research in

a wide range of topics, from large-eddy simulations to the α -mesoscale studies (Cuxart et al., 2000).

A meso- β scale simulation has been performed (with a mesh of 15 km horizontal grid spacing) on a domain surrounding the Paris area. The initial and coupling fields were issued from the French operational forecast model ARPEGE analyses.

To insure a good description of the ABL, 11 levels are taken below 500 m. The thickness of the first 9 meshes is less than 50 m. Above 6400 m, the mesh thickness is constant and set to 500 m. An absorbing layer is set above 15000 m. The top of the domain is located at 21400 m.

For the IOP 2 case study, the simulation starts the on 7 August 1998 at 0000 UTC and ends at on 11 August 1998 at 0000 UTC. In the following, only the Meso-NH model outputs of the 8 August 1998 are shown.

Subsidence was considered to be negligible on 8 August 1998 based on (i) the outputs of the three-dimensional (3D) mesoscale runs performed with Meso-NH (Figure 2) and (ii) the fact that no warming above the ABL (which could have been caused by subsidence) was observed on the Trappes soundings (not shown). After 0900 UTC, vertical velocities are found to be small in the lower 5 km of the troposphere.

Table I shows the estimates of h_{CBL} and h_{RL} retrieved from the lidar reflectivity and from the vertical profiles of potential temperature of the soundings of Trappes and Meso-NH outputs (taken at the base of the temperature inversion). The general agreement is good. However, the use of different techniques to estimate h_{CBL} and h_{RL} from lidar reflectivity and vertical profiles of potential temperature may generate discrepancies (Menut et al., 1999). For instance, a bias of $\simeq 300$ m for h_{RL} is visible between lidar and potential temperature profile estimates, which may be due to the fact that the temperature inversion height does not coincide with the maximum aerosol content (e.g. Dupont, 1991).

Table I. Estimates of h_{CBL} and h_{RL} from lidar and sounding data and from simulation outputs, respectively.

| Time (UTC) | h_{RL} (m) | | | h_{CBL} (m) | | |
|---------------|--------------|----------|---------------|---------------|----------|---------------|
| | Lidar | Sounding | Meso-NH model | Lidar | Sounding | Meso-NH model |
| 0530 | 1600 | 1300 | 1300 | — | — | — |
| 0830 | 1600 | 1400 | 1250 | — | 250 | 300 |
| 1130 | 1450 | — | — | 1100 | 750 | 1000 |
| 1430 | — | — | — | 2050 | 2000 | 2150 |
| 1730 | — | — | — | 2300 | 2350 | 2550 |

At 1130 UTC, the sounding in Trappes shows a temperature inversion at 750 m height which is less than the h_{CBL} heights retrieved from the lidar data and the simulations ($\simeq 1000$ m). This difference may be due to local meteorological effects as Trappes is located approximately 15 km from Palaiseau.

3. Evidence of coupling between the residual and convective boundary layers

3.1. LIDAR MEASUREMENTS

When displayed as a function of time, h_{RL} and h_{CBL} provide useful information on the turbulent activity taking place in the RL and CBL, respectively. From 0800 to 1000 UTC, the height of the top of the RL is nearly constant ($\simeq 1600$ m) which should be an indication of the absence of turbulent motion in the RL. The CBL starts to develop at 1000 UTC and exhibits a fluctuating h_{CBL} with time: the interfacial layer between the mixed layer and the overlying air (either residual layer in the morning, or the free troposphere later) is produced by intermittent turbulent field of thermals leading to downward entrainment of stable air into the CBL. Therefore, as they interact with the capping inversion, updrafts and downdrafts are evidenced by noticeable vertical and horizontal variation of the backscattered signal in this region. Figure 1 shows the presence of thermals interacting with the inversion at the top of the CBL. Simultaneously, we observe similar structures at the top of the RL (Figure 1B). However, it should be noted that because of the so-called "overlap factor", the lidar is not able to retrieve the CBL height below an altitude of 600 m. This could mean that the RL top height starts to fluctuate shortly after the CBL begins to develop. The correlation between the fluctuations of the CBL and RL heights is approximately 80%, which is unexpected if the two layers are disconnected, according to the usual "conceptual" scheme. The RL is eroded by the CBL between 1000 and 1300 UTC. After 1300 UTC, the CBL continues to thicken. The maximum depth observed is 2400 m at 1700 UTC.

Between 1100 and 1300 UTC, we observe a decrease of the lidar reflectivity between 1200 and 1600 m (i.e. in the RL). Simultaneously, the optical depth derived from lidar measurements is constant ($\simeq 0.2$) over the same time period, meaning there is no additional sources of aerosols by synoptic advection or local emissions. The decrease in lidar reflectivity is thus thought to be caused by downward mixing of air

from the free troposphere. The aerosol content in the free troposphere is generally much smaller than in the RL and CBL, so that this vertical mixing results in a reduction of the particle concentration to which the lidar-derived extinction is proportional. This is further confirmed by lidar-derived extinction coefficient time series at 1000, 1450 and 1850 m above ground level, the former two in the RL, the latter above the RL (Figure 3). In the following, lidar-derived extinction coefficients at these heights are referred to as α_{1000} , α_{1450} and α_{1850} . This data is consistent with downward mixing of free tropospheric air (starting at 1100 UTC) for the following reasons

- α_{1000} , α_{1450} and α_{1850} are constant with time prior to 1100 UTC (no downward mixing),
- α_{1000} and α_{1450} diminish significantly at the same time (i.e. 1100 UTC),
- α_{1000} , α_{1450} and α_{1850} are observed to increase significantly at 1200, 1400 and 1530 UTC, respectively, in accordance with the fact that the top of the developing CBL reaches these height at the same time as shown in Figure 1B.

The evidenced mixing process is by nature similar to the entrainment process generally observed at the top of the CBL. However, entrainment results in a deepening of the layer in which the air is entrained: this is observed in the case of the CBL but not in the case of the RL. The height of the RL top is observed to decrease rather than increase (Figure 1B). This is not caused by the detection algorithm since it is a "threshold" algorithm (i.e. the RL is either detected or not detected). Rather, the decrease is thought to be related to a larger entrainment rate at the top of the CBL than at the top of the RL. The CBL and RL growth rates (defined as dh/h , when subsidence is negligible) are equal to 30% and -20% on average between 1100 and 1300 UTC, respectively.

3.2. SIMULATIONS

Theoretically, the dynamical coupling between RL and CBL should also be visible on the vertical profiles of potential temperature. However, the time interval between balloon launches is too large to document accurately the process under scrutiny (between 1000 and 1300 UTC, only one sounding is available). Therefore, we have used meso-scale simulations to provide information on the ABL dynamics within this time interval over Palaiseau area. Figure 4 shows the isentropic contours as a function of time between 0530 and 1730 UTC calculated using 13 potential temperature profiles (one profile every hour). The RL top

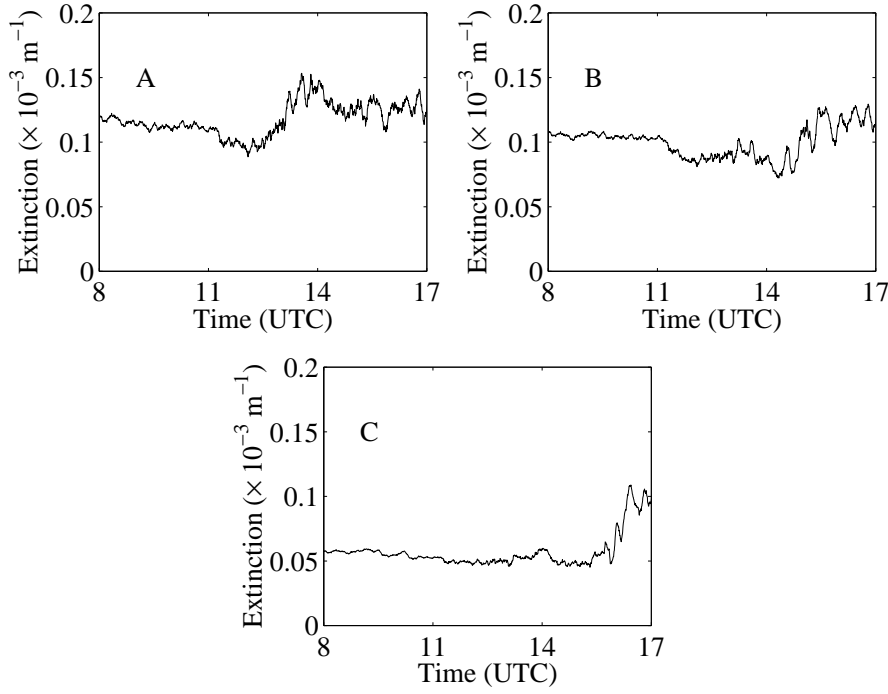


Figure 3. Extinction versus time, derived from backscatter lidar reflectivity, at 1000 m (panel A), 1450 m (panel B) and 1850 m (panel C).

height is located where the potential temperature gradient is maximum, i.e. $\simeq 1500$ m.

Between 0530 and 0800 UTC, the altitude of those isentropes between 304-308 K (in the RL and the free troposphere) increase, most likely because of a slight upward synoptic motion (Figure 2 above 1500 m). On the contrary, they decrease from 0800 to 1200 UTC because of a slight synoptic subsidence (Figure 2 above 1500 m). At 0530 UTC, the isentropes between 304 and 305.5 K are confined between 1000 m and 1600 m. From 0530 to 1030 UTC, the vertical gradient, $\partial\theta/\partial z$ between 305 and 305.5 K isentropes remains relatively constant. On the other hand, the gradient between 304.4 and 304.6 K isentropes decreases, meaning that there is vertical mixing in the RL, which is consistent with lidar observations. Finally, the gradient between 304 and 304.4 K isentropes is observed to increase, as the temperature inversion capping the CBL strengthens.

The top of the vertical isentropes corresponds to the CBL height since vertical isentropes indicate a well mixed layer. The time evolution of the RL and CBL heights is in good agreement with that of h_{RL} and h_{CBL} retrieved from the lidar signals.

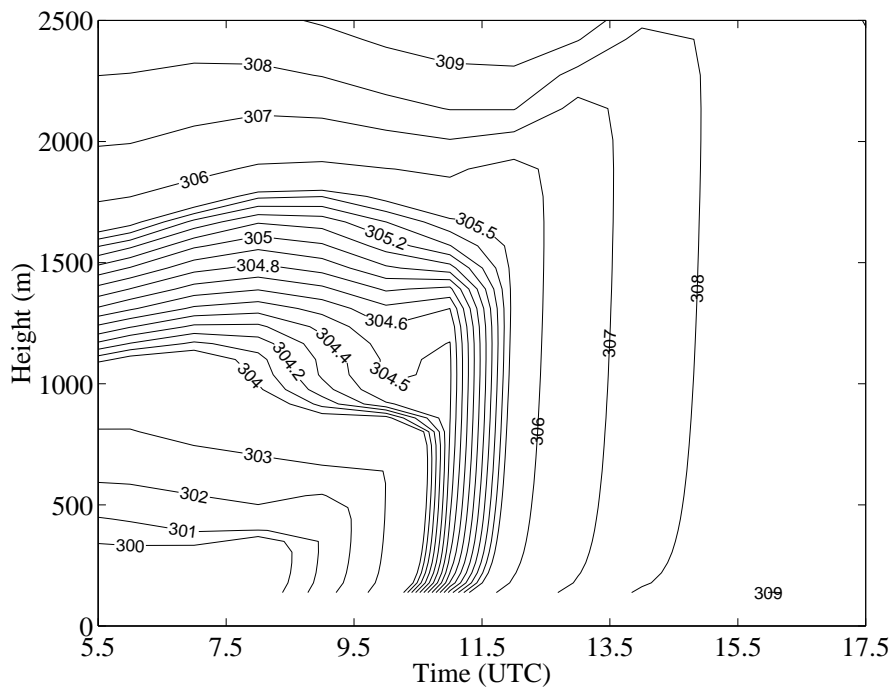


Figure 4. Time series of the vertical profiles of potential temperature at Palaiseau from Meso-NH simulations. Isentropic contour interval is 1 K, except between 304.0 K and 305.5 K where it is equal to 0.1 K.

3.3. DISCUSSION

Horizontal advection of sloping boundaries of the top and bottom of the residual layer layer can also cause apparent changes over a fixed point. Such advection can be significant, even in light wind conditions. Hence, it is important to know the 3D field of mixed layer and residual layer structure, in order to separate the local changes to the advective changes. To address this, we have looked at the horizontal cross sections of height of 304 and 305 K isentropes at 0800, 0900 and 1000 UTC (Figures 5 and 6). This figure strongly advocate against advection as the horizontal structure of the isentropes heights (over Paris and elsewhere) is nearly stationary. Note the sharp boundary (materialized by a height gradient) oriented south-west to north-east (and the associated region, to the south, where the isentropes heights no longer exist) in the lower right corner of the figures. Its southeasterly propagation is related to the growth of the ABL at the mesoscale between 0800 and 1000 UTC.

In Figure 7, we show the vertical structure of the turbulent kinetic energy extracted along an axis parallel to the mean low level wind direction (and going through the Paris area) at 1100 UTC. Paris is

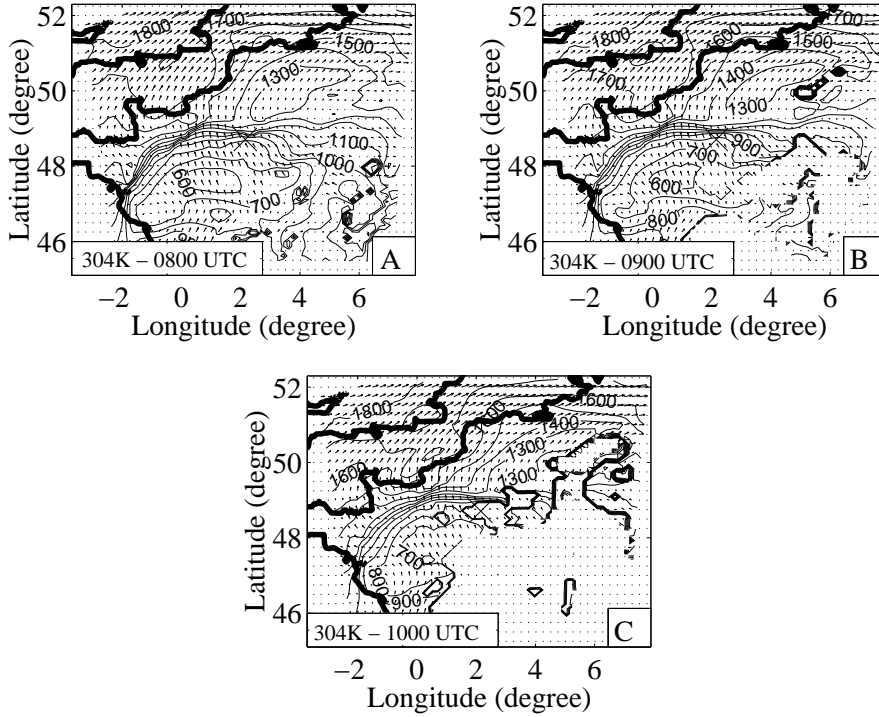


Figure 5. Horizontal cross sections of height of the 304 K isentropic surfaces at 0800 UTC (panel A), 0900 UTC (panel B) and 1000 UTC (panel C). Isopleths are separated by 100 m. The minimum and maximum isocontours are 600 m and 1800 m, respectively. Wind vectors on the isentropic surfaces are superimposed. Paris is indicated by a cross (x).

located 2.35° E, at the lowest point of the topography. Large values of the turbulent kinetic energy are observed over Paris which can unambiguously be related to vertical mixing in the ABL mixed layer.

Between 1100 and 1200 UTC (Figure 8), the depth of the ABL mixed layer increases significantly under the influence of surface heating. Nevertheless, some of this increase could be caused by entrainment at the top of the RL. However, this cannot be evidenced with the present simulation (not because the vertical resolution is too coarse). We believe that with a mesh of 15 km horizontal grid spacing the TKE scheme in the model is not appropriate to separate the TKE generated by the entrainment at the top of the RL and that created by entrainment at the top of the CBL. This would need to be studied with a large-eddy simulation model.

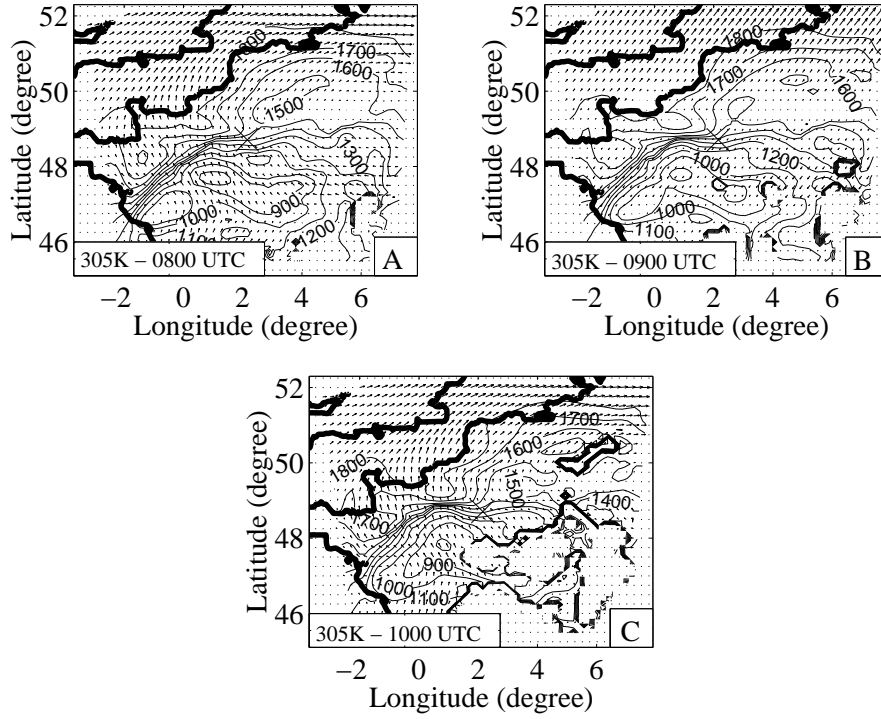


Figure 6. Same as Figure 5 for the 305 K isentropic surfaces.

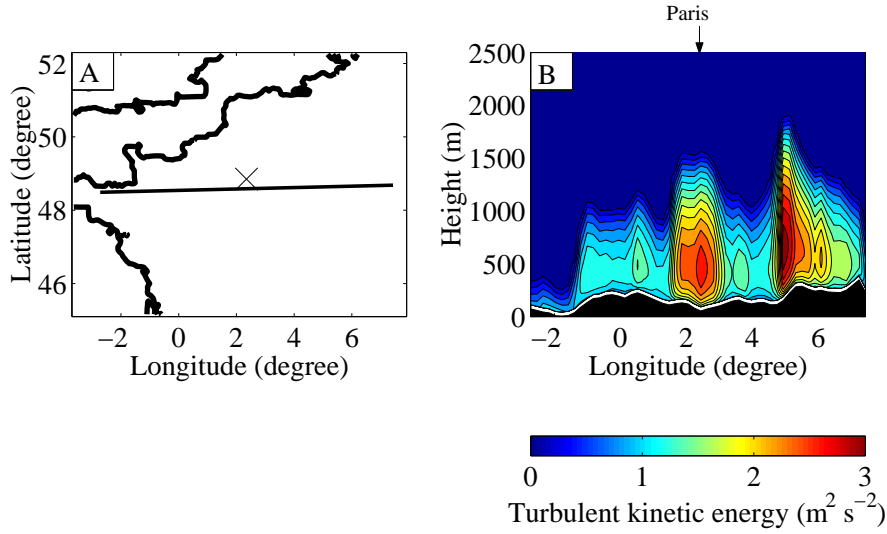


Figure 7. Vertical structure of the turbulent kinetic energy (panel B) extracted along an axis parallel to the mean low level wind direction (panel A) at 1100 UTC. Paris is indicated by a cross (x) in panel A and by an arrow in panel B.

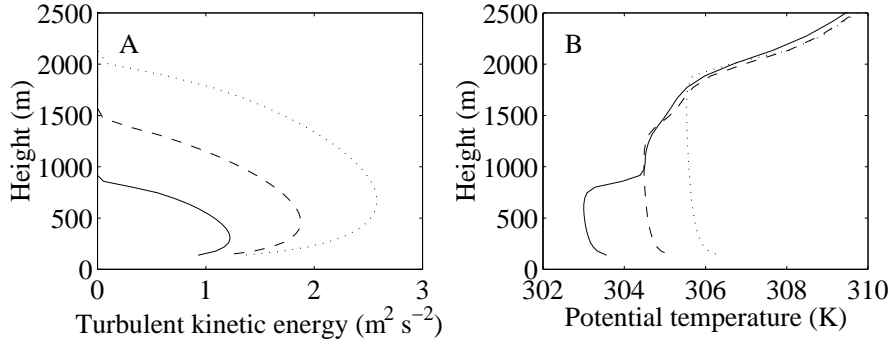


Figure 8. Simulation of the vertical profiles of turbulent kinetic energy (panel A) and potential temperature (panel B) in Palaiseau at 1000, 1100 and 1200 UTC (solid, dashed and dotted line, respectively).

4. Conclusion

In the present study, turbulence in the RL has been observed using a ground-based lidar by looking at the fluctuations, with time, of the height of the RL top. [Such fluctuations are known to be related to interactions between thermals and the inversion capping the CBL via wave propagation and turbulence.]

The turbulence in the RL is likely to be of different origin than in the CBL. It could be generated by wind-shear (however, this generally leads to downward mixing). It could also be produced by so-called "convective" gravity waves resulting from the interaction between the flow in the RL and thermals deforming the top of the CBL. Convective gravity waves transport momentum upward which, in turn, leads to enhanced drag and mixing. Such waves could have an impact on atmospheric circulation as discussed by Kershaw (1995). Lidar measurements strongly advocate for the later hypothesis, since the RL top height starts to fluctuate shortly after the CBL begins to develop.

The concept of bidirectional entrainment in an "intermediate" layer (i.e. the entrainment of fluid from both the underlying ABL and the overlying free troposphere into a layer between the ABL and the free troposphere) has been studied theoretically (Fernando and Hunt, 1997), via laboratory experiments (Turner, 1968; McGrath et al., 1997) as well as experimentally in the framework of the First Aerosol Characterization Experiment (ACE 1) by Russell et al. (1998). According to these studies, bidirectional entrainment is to be expected whenever turbulence is present in the "intermediate" layer (here, a portion of the top of the RL). This advocates against the generally accepted concept of

a constant RL top height overnight (if we except the effect of subsidence and radiative cooling).

Further investigations will be conducted with a large-eddy simulation model to explain the difference of CBL and RL growth rates (30% and -20% on average, respectively) and the role of convective gravity waves.

Acknowledgements

The authors would like to thank Laurent Menut for providing the data from the Trappes balloon soundings made during ESQUIF. ESQUIF has been funded by the Institut Pierre-Simon Laplace (IPSL), the Ministère de l'Aménagement du Territoire et de l'Environnement, the Conseil Régional d'Ile-de-France, the Commissariat à l'Energie Atomique, and Elf-Aquitaine. This work has been supported by CNRS and CNES. The authors would like to thank the anonymous reviewers for their comments and suggestions.

References

- Bélair, S., Lacarrère, P., Noilhan, J., Masson V., and Stein, J.: 1998, 'High-Resolution Simulation of Surface and Turbulent Fluxes during HAPEX-MOBILHY', *Mon. Wea. Rev.* **126**, 2234-2253.
- Cuxart, J., Bougeault, P., and Redelsperger J.-L.: 2000, 'A Turbulence Scheme Allowing for Mesoscale and Large-eddy Simulations', *Quart. J. Roy. Meteorol. Soc.* **126**, 1-30.
- Devara, P. S. C., Raj, P. E., and Sharma, S.: 1994, 'Remote Sensing of Atmospheric Aerosol in the Nocturnal Boundary Layer', *Environ. Pollut.*, **85**, 97-102.
- Di Girolamo P., Ambrico, P. F., Amodeo, A., Boselli, A., Pappalardo, G., and Spinelli, N.: 1999, 'Aerosol Observations by Lidar in the Nocturnal Boundary Layer', *Appl. Opt.*, **38**, 4585-4595.
- Drobinski, P., Brown, R. A., Flamant, P. H., and Pelon, J.: 1998, 'Evidence of Organized Large Eddies by Ground-Based Doppler Lidar, Sonic Anemometer and Sodar', *Boundary-Layer Meteor.*, **88**, 343-361.
- Drobinski, P., Flamant, C., Dusek, J., Pelon, J., and Flamant, P. H.: 2001, 'Observational Evidence and Modeling of an Internal Hydraulic Jump at the Atmospheric Boundary Layer Top During a Tramontane Event', *Boundary-Layer Meteor.*, in press.
- Dupont, E.: 1991, 'Etude Méthodologique et Expérimentale de la Couche Limite Atmosphérique par Télédétection Laser', Ph. D. Thesis, Université Pierre et Marie Curie, Paris, France, 220 pp.
- Dupont, E., Pelon, J. and Flamant, C.: 1994, 'Study of the Moist Convective Boundary Layer Structure by Backscatter Lidar', *Bound.-Layer Meteor.* **69**, 1-25.
- Dupont E., Menut, L., Carissimo, B., Pelon, J., and Flamant, P. H.: 1997, 'Comparison Between the Atmospheric Boundary Layer in Paris and its Rural Suburbs during the ECLAP Experiment', *Atmos. Environ.* **33**, 979-994.

- Fernando, H. J. S., and Hunt, J. C. R.: 1997, 'Turbulence, Waves and Mixing at Shear-free Density Interfaces, 1, A Theoretical Model', *J. Fluid Mech.* **347**, 197-234.
- Flamant, C., and Pelon, J.: 1996, 'Atmospheric Boundary-Layer Structure Over the Mediterranean During a Tramontane Event', *Quart. J. Roy. Meteorol. Soc.* **122**, 1741-1778.
- Flamant, C., Pelon, J., Flamant, P. H., and Durand, P.: 1997, 'Lidar Determination of the Entrainment Zone Thickness at the Top of the Unstable Marine Atmospheric Boundary-Layer', *Bound.-Layer Meteor.* **83**, 247-284.
- Flamant, C., Trouillet, V., Chazette, P., and Pelon, J.: 1998, 'Wind Speed Dependence of Atmospheric Boundary Layer Optical Properties and Ocean Surface Reflectance as Observed by Backscatter Lidar', *J. Geophys. Res.* **103**, C11, 25,137-25,158.
- Kershaw, R.: 1995, 'Parametrization of Momentum Transport by Convectively Generated Gravity Waves', *Quart. J. Roy. Meteorol. Soc.* **121**, 1023-1040.
- Kolev, I., Savov, P., Kaprielov, B., Parvanov, O., and Simeonov, V.: 2000, 'Lidar Observation of the Nocturnal Boundary Layer Formation over Sofia, Bulgaria', *Atmos. Environ.* **34**, 3223-3235.
- Lafore, J. P., Stein, J., Asencio, N., Bougeault, P., Ducrocq, V., Duron, J., Fischer, C., Hérel, P., Mascart, P., Masson, V., Pinty, J. P., Redelsperger, J. L., Richard, E., and Vilà-Guerau de Arellano, J.: 1998, 'The Meso-Nh Atmospheric Simulation System. Part I: Adiabatic Formulation and Control Simulation', *Ann. Geophys.* **16**, 90-109.
- Mahrt, L.: 1981, 'The Early Evening Boundary Layer Transition', *Quart. J. Roy. Meteorol. Soc.* **107**, 329-343.
- Mahrt, L.: 1999, 'Stratified Atmospheric Boundary Layers', *Bound.-Layer Meteor.* **90**, 375-396.
- McGrath, J. L., Fernando, H. J. S., and Hunt, J. C. R.: 1997, 'Turbulence, Waves and Mixing at Shear-free Density Interfaces, 2, Laboratory Experiments', *J. Fluid Mech.* **347**, 235-261.
- Menut, L., Flamant, C., Pelon, J., and Flamant, P. H.: 1999, 'Urban Boundary Layer Height Determination from Lidar Measurements over the Paris Area', *Appl. Opt.*, **38**, 945-954.
- Menut, L., Vautard, R., Flamant, C., Abonne, C., Beekmann, M., Chazette, P., Flamant, P. H., Gombert, D., Guedalia, D., Kley, D., Lefebvre, M. P., Lossec, B., Martin, D., Megie, G., Sicard, M., Perros, P., and Toupance, G.: 2001, 'Atmospheric Pollution over the Paris Area: The ESQUIF Project', *Ann. Geophys.*, in press.
- Neu, U., Künzle, T., and Wanner, H.: 1994, 'On the Relation Between Ozone Storage in the Residual layer and Daily Variation in the Near-surface Ozone Concentration- A Case Study', *Bound.-Layer Meteor.* **69**, 221-247.
- Nieuwstadt, F. T. M., and Brost, R. A.: 1986, 'The Decay of Convective Turbulence', *J. Atmos. Sci.* **43**, 532-546.
- Raj, P. E., Devara, P. S. C., Mahes Kumar, R. S., Pandithurai, G., and Dani, K. K.: 1997, 'Lidar Measurements of Aerosol Column Content in an Urban Nocturnal Boundary Layer', *Atmos. Res.*, **45**, 201-216.
- Russell, L. M., Lenschow, D. H., Laursen, K. K., Krummel, P. B., Siems, S. T., Bandy, A. R., Thornton, D. C., and Bates, T. S.: 1998, 'Bidirectional Mixing in an ACE 1 Marine Boundary Layer Overlain by a Second Turbulent Layer', *J. Geophys. Res.* **103**, D13, 16,411-16,432.

- Stull, R.B.: 1988, 'An Introduction to Boundary Layer Meteorology', Kluwer Academic Publishers, 666p.
- Turner, J. S.: 1968, 'The Influence of Molecular Diffusivity on Turbulent Entrainment Across a Density Interface', *J. Fluid Mech.* **33**, 639-656.
- Wilczak, J. M., Gossard, E. E., Neff, W. D., and Eberhard, W. L.: 1996, 'Ground-based Remote Sensing of the Atmospheric Boundary Layer: 25 Years of Progress', *Bound.-Layer Meteor.* **78**, 321-349.